Oscillatory double-diffusive convection in a rotating spherical shell at high Rayleigh numbers

Yue-Kin Tsang

School of Mathematics, Statistics and Physics
Newcastle University

Céline Guervilly
Graeme R. Sarson

Oscillatory double-diffusive convection (semi-convection)

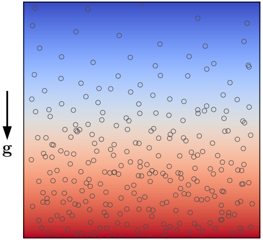

- Double-diffusive convection: density variation comes from two different scalars, T and C
- Consider a heavy element in the fluid, e.g. salt in seawater, He in H–He mixture
- Let C be the concentration of the heavy element, then:

$$\rho(T, C) = \rho_m \left[1 - \alpha_T (T - T_m) + \alpha_C (C - C_m)\right], \quad \alpha_T, \alpha_C > 0$$

- What distinguishes T and C is their diffusivities: $\kappa_T \gg \kappa_C$
- **ODDC**: temperature (fast diffusing) is destabilising, composition is stablising
- Rayleigh numbers: thermal $Ra_T > 0$, compositional $Ra_C < 0$

Possible scenarios of ODDC in planetary and stellar interiors

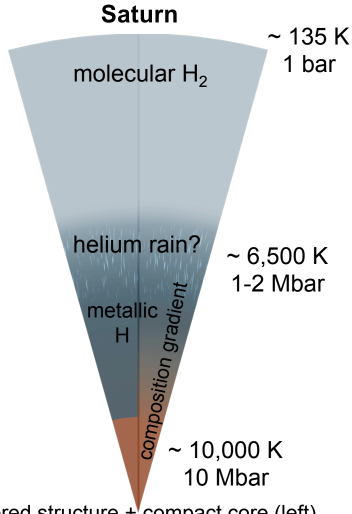

layered structure + compact core (left), inhomogeneous structure + fuzzy core (right)

- Stabilising compositional gradient may form inside Saturn in two different ways:
  - helium rain: at some specific temperature and pressure, H and He become immiscible, heavy He droplets falls inwards and accumulates above the deep interior (*Salpeter 1973; Stevenson & Salpeter 1977*)
  - dilute/fuzzy core: recent observations suggest the existence of an extended stably stratified region created by heavy elements dissolving from a compact inner core (*Mankovich & Fuller 2021*)
- Composition gradient, and thus ODDC, may also exist in:
  - Jupiter
  - core-convective main sequence stars

Fortney et al. in "Saturn: The Grand Finale", K. H. Baines et al., eds., Cambridge University Press

Mathematical model: ODDC in a rotating spherical shell

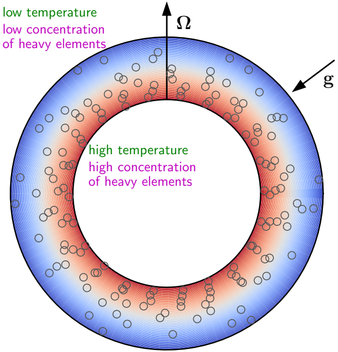

Boundary condition

fixed T gradient:

$$\left.\frac{\partial T}{\partial r}\right|_{r_i}, \left.\frac{\partial T}{\partial r}\right|_{r_o} < 0$$

fixed C gradient:

$$\left.\frac{\partial C}{\partial r}\right|_{r_i}, \left.\frac{\partial C}{\partial r}\right|_{r_o} < 0$$

Equilibrium profiles (at $\boldsymbol{u} = 0$)

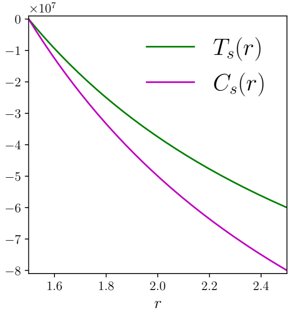

$$\frac{\mathrm{d}T_s}{\mathrm{d}r} < 0 \quad \textit{destabilising}$$

$$\frac{\mathrm{d}C_s}{\mathrm{d}r} < 0 \quad \textit{stabilising}$$

$$\rho(T_s, C_s) = \rho_m[1 - \alpha_T(T_s - T_m) + \alpha_C(C_s - C_m)]$$

Consider a Boussinesq fluid in a rotating spherical shell of inner radius r_i and outer radius r_o

- (equilibrium) buoyancy frequency: $N_0^2 = -\dfrac{g}{\rho_m}\dfrac{\mathrm{d}}{\mathrm{d}r}\rho(T_s, C_s) \implies N_0^2 = g\alpha_T\dfrac{\mathrm{d}T_s}{\mathrm{d}r} - g\alpha_C\dfrac{\mathrm{d}C_s}{\mathrm{d}r}$
- inverse density ratio: $R_\rho^{-1} = \dfrac{\alpha_C|\mathrm{d}C_s/\mathrm{d}r|}{\alpha_T|\mathrm{d}T_s/\mathrm{d}r|}$

Governing equations

Non-dimensional equations:

$$\frac{\partial \boldsymbol{u}}{\partial t} + (\boldsymbol{u}\cdot\nabla)\boldsymbol{u} + \frac{2}{Ek}\hat{\boldsymbol{z}}\times\boldsymbol{u} = -\nabla\Pi + (\Theta - \xi)r\,\hat{\boldsymbol{r}} + \nabla^2\boldsymbol{u},$$

$$\nabla\cdot\boldsymbol{u} = 0,$$

$$\frac{\partial\Theta}{\partial t} + \boldsymbol{u}\cdot\nabla\Theta = \frac{Ra_T}{Pr}\left(\frac{\Gamma}{1-\Gamma}\right)^2\frac{u_r}{r^2} + \frac{1}{Pr}\nabla^2\Theta, \quad \Theta(\boldsymbol{x},t) = T(\boldsymbol{x},t) - T_s(r)$$

$$\frac{\partial\xi}{\partial t} + \boldsymbol{u}\cdot\nabla\xi = \frac{|Ra_C|}{Sc}\left(\frac{\Gamma}{1-\Gamma}\right)^2\frac{u_r}{r^2} + \frac{1}{Sc}\nabla^2\xi, \quad \xi(\boldsymbol{x},t) = C(\boldsymbol{x},t) - C_s(r)$$

Dimensionless numbers:

$$\Gamma = \frac{r_i}{r_o} = 0.6, \quad Ek = \frac{\nu}{\Omega D^2} = 10^{-4}, \quad \text{(small)}\ Pr = \frac{\nu}{\kappa_T} = 0.3, \quad Sc = \frac{\nu}{\kappa_C} = 3 \quad \left(\tau = \frac{\kappa_C}{\kappa_T} = 0.1\right)$$

$$Ra_T = \frac{g_o\alpha_T D^5}{r_o\nu\kappa_T}\left|T_s'(r_i)\right| \quad \text{and} \quad Ra_C = -\frac{g_o\alpha_C D^5}{r_o\nu\kappa_C}\left|C_s'(r_i)\right|$$

Numerical simulations using XSHELLS by Nathanaël Schaeffer (Université Grenoble Alpes)

Phase diagram: top-heavy vs. bottom heavy

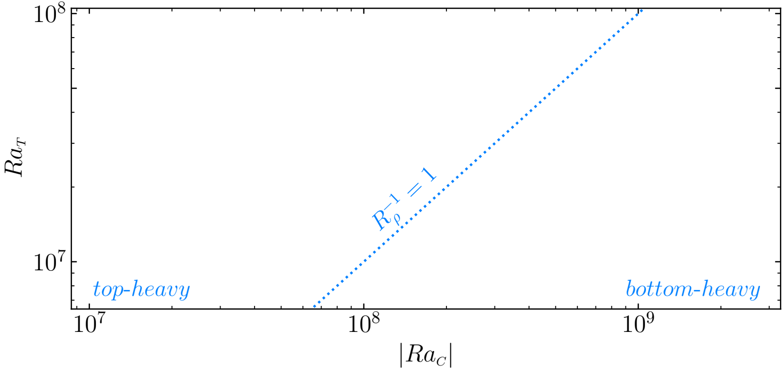

- $N_0^2 = -\dfrac{Ra_T}{Pr}\dfrac{r_i^2}{r} + \dfrac{|Ra_C|}{Sc}\dfrac{r_i^2}{r}$, $\quad N_0^2 < 0$: unstable stratification, $N_0^2 > 0$: stable stratification
- $R_\rho^{-1} = \dfrac{\tau |Ra_C|}{Ra_T}$, $\quad R_\rho^{-1} < 1$: unstable stratification, $R_\rho^{-1} > 1$: stable stratification
- critical Rayleigh number for pure thermal convection $\approx 1.77 \times 10^5$

Phase diagram: global stability

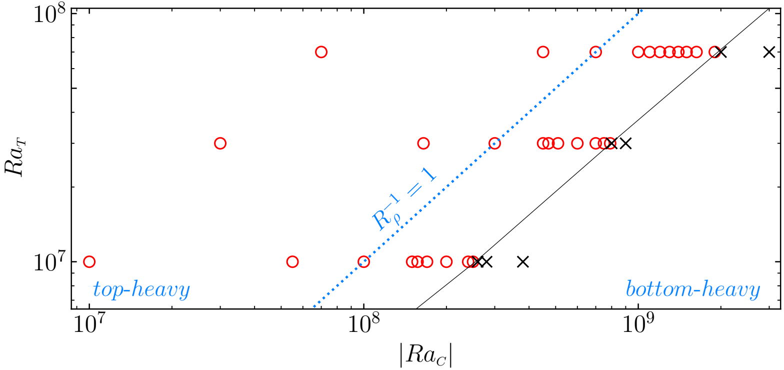

black crosses ($\times$): stable   red circles ($\circ$): unstable

- Three different Ra_T and varies Ra_C
- Convection occurs for $R_\rho^{-1} < 1$ *(overturning convection)*
- Convection occurs for $R_\rho^{-1} > 1$ at some moderately large $|Ra_C|$ *(double-diffusive effect)*
- For a given Ra_T, system is stable when R_ρ^{-1} (or $|Ra_C|$) is larger than some critical value

Kinetic energy

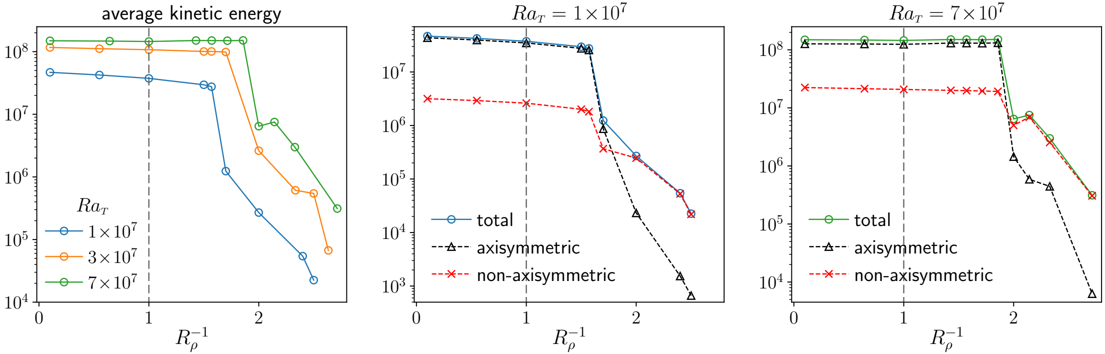

For a given Ra_T:

- KE remains roughly constant for R_ρ^{-1} less than some threshold $R_* > 1$ $(R_\rho^{-1} = \tau|Ra_C|/Ra_T)$
- KE drops sharply at $R_\rho^{-1} \approx R_*$ and remains small for $R_\rho^{-1} > R_*$
- $R_\rho^{-1} < R_*$: KE is dominated by the axisymmetric $(m = 0)$ velocity
- $R_\rho^{-1} > R_*$: KE is dominated by the non axisymmetric $(m \neq 0)$ velocity

Field morphology: thermal-like behaviour

$Ra_T = 3 \times 10^7$, $Ra_C = -4.5 \times 10^8$

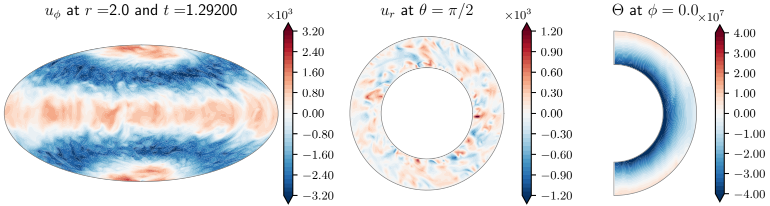

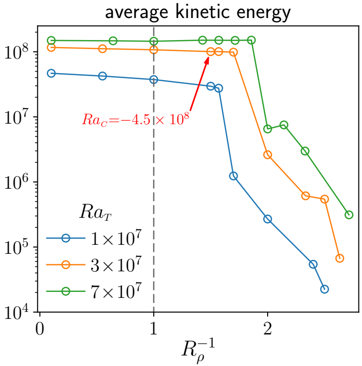

- similar to pure thermal (overturning) convection—even though $R_\rho^{-1} > 1$

Field morphology: comparing to pure thermal convection

$Ra_T = 3 \times 10^7$, $Ra_C = -4.5 \times 10^8$

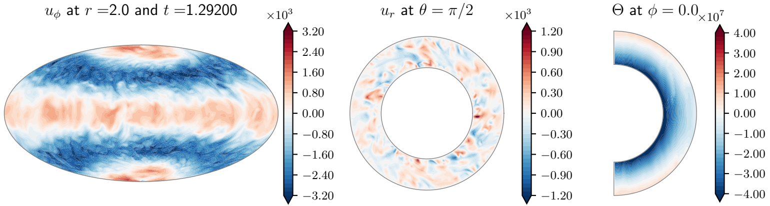

- similar to pure thermal (overturning) convection—even though $R_\rho^{-1} > 1$

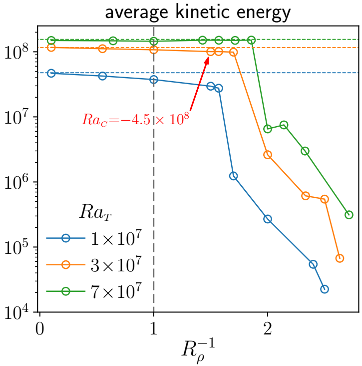

Pure thermal convection at $Ra_T = 3 \times 10^7$

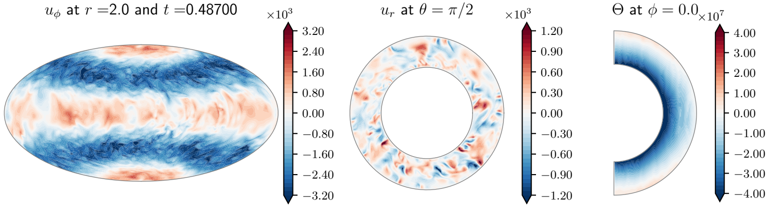

- pure thermal convection ($R_\rho^{-1} = 0$)

Field morphology: oscillatory double-diffusive behaviour

$Ra_T = 3 \times 10^7,\ Ra_C = -4.5 \times 10^8$

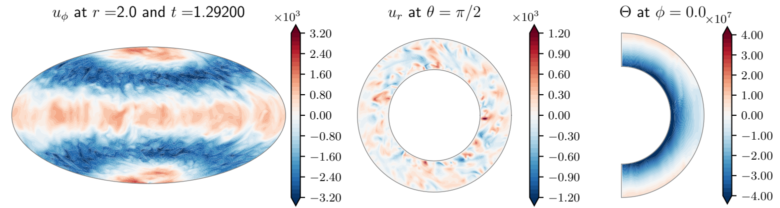

- similar to pure thermal (overturning) convection—even though $R_\rho^{-1} > 1$

$Ra_T = 3 \times 10^7,\ Ra_C = -7.5 \times 10^8$

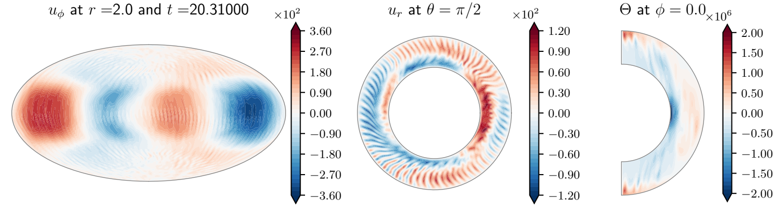

- overlapping of large-scale pattern and small-scale wave motions

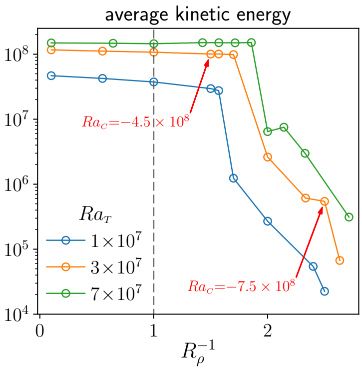

Buoyancy frequency ($Ra_T = 3 \times 10^7$)

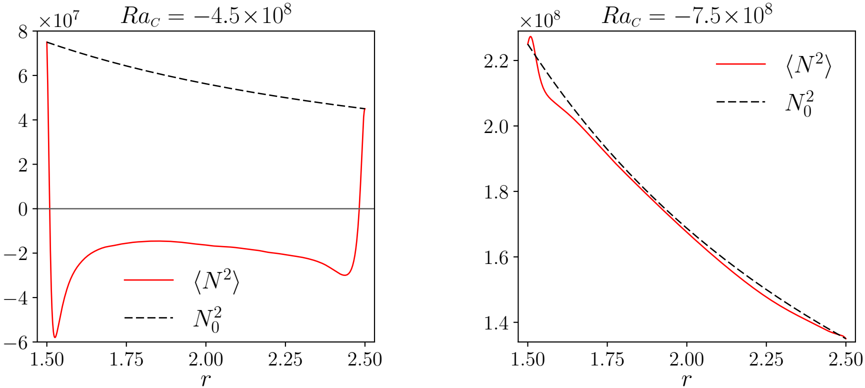

Equilibrium: $$N_0^2 = g\alpha_T \frac{\mathrm{d}T_s}{\mathrm{d}r} - g\alpha_C \frac{\mathrm{d}C_s}{\mathrm{d}r}\,,$$ $N_0^2 > 0$ for both cases

Statistically steady: $$\langle N^2 \rangle = g\alpha_T \frac{\mathrm{d}\langle T\rangle}{\mathrm{d}r} - g\alpha_C \frac{\mathrm{d}\langle C\rangle}{\mathrm{d}r}\,,$$ $$\langle f\rangle = \int \left[\frac{1}{4\pi}\int_0^{2\pi}\int_0^{\pi} f(r,\theta,\phi,t)\,\mathrm{d}\theta\mathrm{d}\phi\right]\mathrm{d}t$$

Force balance $(Ra_T = 3 \times 10^7)$

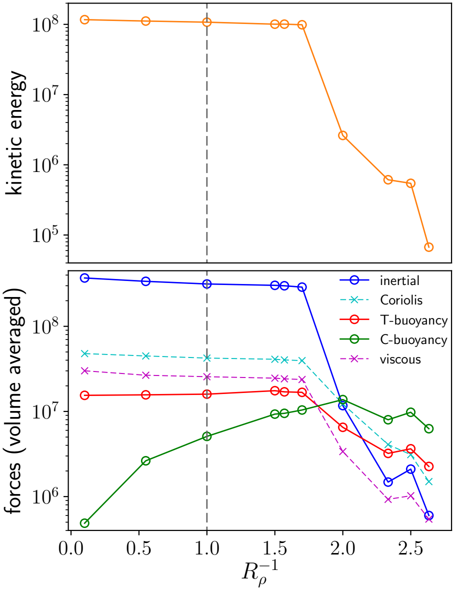

$$\frac{\partial \boldsymbol{u}}{\partial t} + \underbrace{(\boldsymbol{u}\cdot\nabla)\boldsymbol{u}}_{\text{inertia}} + \underbrace{\frac{2}{Ek}\hat{\boldsymbol{z}}\times\boldsymbol{u}}_{\text{Coriolis}} = -\nabla\Pi + \underbrace{\Theta\, r\,\hat{\boldsymbol{r}}}_{\text{thermal buoyancy}} - \underbrace{\xi\, r\,\hat{\boldsymbol{r}}}_{\text{compositional buoyancy}} + \underbrace{\nabla^2\boldsymbol{u}}_{\text{viscous}}$$

- transition occurs near $R_\rho^{-1} = R_*$ where the strengths of thermal buoyancy and compositional buoyancy are comparable

Summary

- $R_\rho^{-1} < 1 \ \ (N_0^2 < 0)$:
  - Compositional buoyancy negligible
  - Thermal-like overturning convection
- $1 < R_\rho^{-1} < R_* \ \ (N_0^2 > 0)$:
  - Compositional buoyancy increasing, but ...
  - Thermal-like overturning convection persists
- $R_\rho^{-1} \approx R_* \ \ (N_0^2 > 0)$: thermal buoyancy $\sim$ compositional buoyancy
- $R_\rho^{-1} > R_* \ \ (N_0^2 > 0)$:
  - Compositional buoyancy $>$ thermal buoyancy
  - Oscillatory double-diffusive behaviour before the system becomes stable at large R_ρ^{-1}
- Dynamo at $R_\rho^{-1} > 1$? Yes.
  Dynamo at $R_\rho^{-1} > R_*$? *Yes!*